Silver, titanium dioxide and zinc oxide nanoparticles trigger miRNA/isomiR expression changes in THP-1 cells that are proportional to their health hazard potential.

Joseph Ndika[a,*], Umair Seemab[a,#], Wing-Lam Poon[b,#], Vittorio Fortino[c], Hani El-Nezami[b,d], Piia Karisola[a] and Harri Alenius[a,e]

[a]Human Microbiome Research Program, Faculty of Medicine, University of Helsinki; [b]School of Biological Sciences, The University of Hong Kong, Hong Kong; [c]Institute of Biomedicine, University of Eastern Finland, Kuopio, Finland; [d]Institute of Public Health and Clinical Nutrition, School of Medicine, University of Eastern Finland, Kuopio, Finland; [e]Institute of Environmental Medicine (IMM), Karolinska Institutet, Stockholm, Sweden

[*]Correspondence: Systems Immunology Group, Department of Bacteriology and Immunology, Medical Faculty, University of Helsinki, Haartmaninkatu 3, FIN-00014 Helsinki, Finland.
email: joseph.ndika@helsinki.fi

[#]Contributed equally

Running title:
miRnomics of metal-based nanoparticle exposure in an immune cell model

Silver, titanium dioxide and zinc oxide nanoparticles trigger miRNA/isomiR expression changes in THP-1 cells that are proportional to their health hazard potential.

Abstract

After over a decade of nanosafety research, it is indisputable that the vast majority of nano-sized particles induce a plethora of adverse cellular responses - the severity of which is linked to the material's physicochemical properties. Differentiated THP-1 cells were previously exposed for 6 hours (6h) and 24 hours (24h) to silver, titanium dioxide and zinc oxide nanoparticles at the maximum molar concentration at which no more than 15% cellular cytotoxicity was observed. All three nanoparticles differed in extent of induction of biological pathways corresponding to immune response signaling and metal ion homeostasis. In the current study, we integrated gene and miRNA expression profiles from the same cells to propose miRNA biomarkers of adverse exposure to metal-based nanoparticles. We employed RNA sequencing together with a quantitative strategy that also enables analysis of the overlooked repertoire of length and sequence miRNA variants called isomiRs. Whilst only modest changes in expression was observed within the first 6h of exposure, the miRNA/isomiR (miR) profiles of each nanoparticle was unique. Via canonical correlation and pathway enrichment analyses, we identified a co-regulated miR-mRNA cluster, predicted to be highly relevant for cellular response to metal ion homeostasis. These miRs were annotated to be canonical or variant isoforms of Hsa-miR-142-5p, -342-3p, -5100, -6087, -6894-3p and -7704. Hsa-miR-5100 was differentially expressed in response to each nanoparticle in both the 6h and 24h exposures. Taken together, this co-regulated miR-mRNA cluster could represent potential biomarkers of sub-toxic metal-based nanoparticle exposure.

Keywords

Metal-based nanoparticle, bio-nano reactivity, miRNA, isomiR

Introduction

In recent years, much progress has been made in the field of nanotechnology towards the development of different kinds of nanomaterials with a wide range of applications. Because of their size, nanoparticles can cross cell membranes, and this makes them a significant health hazard if they are inhaled, ingested or cross the skin barrier. Additionally, the same configurable physicochemical properties that confer industrial and biomedical relevance to nanomaterials, are directly related to their health hazard potential (Hristozov et al. 2012). As a result, previous regulatory indications stipulated that health risk assessment should be done for each individual nanoform variant of size, shape, surface chemistry, etc. (for example, SCENIHR, 2009; EFSA Scientific Committee, 2011). However, it is now recognized that the extent of animal experimentation, time and money required to completely characterize the vast array of existing and upcoming nanomaterial configurations is just not realistic (Hristozov et al. 2016). The increasing revenue of nanotechnology directly translates to increasing human and environmental contact with nanoparticles, and with it, adverse health effects. More than ever, comprehensive tools to assess implementation of protective measures, diagnose early exposures and predict hazardous novel nanoparticles are needed.

When subjected to environmental perturbations, cells and organisms mount a coordinated molecular response that is of homeostatic, pathologic or evolutionary importance. Therefore, profiling changes in gene and protein expression within the context of toxicant exposure, leading to mechanistic information on how biological networks are perturbed as a function of specific nanoparticle features, constitutes a paradigm shift from a material-by-material approach, to predictive classification of hazardous nanomaterials based on shared features (Fadeel et al. 2018). This is especially important because nanoparticles can for example be classified according to their composition as being carbon-based, metal or metal oxide based and inorganic. As such, in addition to hazard identification and classification of nanomaterials, omics-based approaches can also be used to develop biomarkers of adverse exposures to a range of nanoparticles that can be grouped into a specific class.

The magnetic and antimicrobial properties of metal and metal oxide nanoparticles makes them highly desirable in medicine and industry. Silver (Ag), titanium dioxide (TiO_2) and zinc oxide (ZnO) nanoparticles, are the most common metal-based nanoparticles with a combined yearly production of up to 6600 tons per year (Piccinno et al. 2012). These three nanoparticles currently represent 47% of nano-enabled consumer products with known nanoparticle compositions that have been registered in the ERC-funded *nanodb* database (www.nanodb.dk). TiO_2 and ZnO nanoparticles are predominantly used in sunscreens and cosmetic products, and the majority of consumer products registered to contain Ag nanoparticles are personal care, clothing and cleaning products (www.nanodb.dk, accessed December 2018). Ag, TiO_2 and ZnO are also amongst the most common nanomaterials used in food products (Contado 2015). There is thus a significant potential for uncontrolled human exposure (via inhalation during for example production, or through the skin) to these types of nanoparticles and studies investigating biomarkers of adverse exposure are thus warranted.

We previously implemented microarray-based mRNA expression profiling, to characterize early immune responses in viability-normalized (maximum 15% cell death) differentiated THP-1 cells after 6 hours (6h) and 24 hours (24h) exposures to polyvinylpyrrolidone-coated silver, titanium dioxide and zinc

oxide nanoparticles (nAg, $nTiO_2$ and nZnO) (Poon et al. 2017). Therein, in addition to a distinct upregulation of a cluster of metallothionein genes, we observed induction of an antiviral-type response in nAg- and nZnO-, but not $nTiO_2$-exposed cells. In order to further understand common and distinguishable mechanisms that govern the cellular reactivities of nAg, $nTiO_2$ and nZnO, we have now proceeded to characterize the repertoire of microRNAs (miRNome) from total RNA derived from the same THP-1 cells. We hypothesized that, the toxicological potential of each particle will be reflected by a typical miRNA profile from whence biomarkers of specific or common mechanism(s) of toxicity can be identified.

It has recently emerged that the distinct length and sequence variants of canonical miRNAs (collectively known as isomiRs) (Neilsen, Goodall, and Bracken 2012) which are frequently identified via small RNA sequencing, increase the diversity and functionality of the miRNome (Gebert and MacRae 2018). Differential miRNA expression in response to nanoparticle exposure has been reported in a few studies (reviewed in (Shyamasundar et al. 2015; Wong, Hu, and Baeg 2017)), but in comparison to mRNA, miRNAs and other non-coding RNAs have received very little attention and there is a gap in understanding the effect of nanoparticles on this part of the (epi)genome. Furthermore, because the concept of functionally distinct isomiRs is relatively novel, previous studies investigating miRNA changes in response to nanoparticle exposure have often used quantitative approaches that aggregate counts from near identical sequences (Stokowy et al. 2014). In this study, we have used a quantitative pipeline that emphasizes on identifying known miRNAs (miRBase repository) and all their stably expressed sequence variants, to investigate the cross-talk between nanoparticle type, mRNA and miRNA expression. We leverage an experimental set-up wherein a cell line model of the immune system was exposed to industry-relevant nanoparticles normalized to the same biological effect dose (i.e. maximum molar concentrations that do not cause more than 15% cellular cytotoxicity), to investigate material-specific immune responses.

Materials and Methods

The described study is based on small RNAseq of total small RNA purified from previously isolated total RNA of differentiated THP-1 cells exposed for 6 hours (6h) or 24 hours (24h) to silver, titanium dioxide and zinc oxide nanoparticles (nAg, $nTiO_2$ and nZnO). The particle characteristics provided by the manufacturers, as well as experimentally determined hydrodynamic sizes and surface charge in complete RPMI medium (cRPMI) are outlined in Table 1. Nano-sized rutile/anatase (90/10%) titanium dioxide (TiO_2 30-40nm, NanoAmor, 5485HT) and zinc oxide (ZnO 20 nm, NanoAmor, 5810MR) were purchased from Nanostructured & Amorphous Materials, Inc. (Houston, USA). Nano-sized PVP-coated silver in water (BioPure Silver Nanospheres – PVP, 20 nm / 1 mg/ml water / 1 ml, SKU: AGPB20-1M) was purchased from NanoComposix, (San Diego, USA). All cell lines were purchased from American Type Culture Collection (ATCC, Rockville, MD, USA). Experimental details pertaining to particle dispersion, dosimetry modelling, cell exposures and microarray-based mRNA profiling have been previously described (Poon et al. 2017). A brief overview of the cell exposure is provided below.

Exposure

THP-1 cells are human leukemia monocytic cells that grow in suspension. They were differentiated into adherent macrophage-like cells by culturing them for 48 hours in growth media supplemented with 50 nM phorbol-12-myristate-13-acetate (PMA). Differentiated THP-1 cells were then exposed to nanoparticles at a dose corresponding to the maximum nanoparticle concentration at which less than 15% cell death was observed. The nanoparticle doses at which greater than 85% cell viability was retained, was determined with the MTT tetrazolium assay, as described previously. This was, 10 µg/ml (6 µg/cm^2) for Ag and ZnO nanoparticles, and 100 µg/ml (60 µg/cm^2) for TiO_2 nanoparticles (Poon et al. 2017). Nanoparticles were added to cell cultures of PMA-differentiated THP-1 cells, and incubated under standard cell conditions for 6 hours and 24 hours. To validate the expression of selected miRNAs across cell types, A549 cells were exposed to the same concentration (10 µg/ml) of Ag nanoparticles, for 24 hours. Prior to nanoparticle exposures, A549 cells were cultured to 70% confluence, in complete RPMI, supplemented with 10% heat-inactivated FBS and 1% penicillin-streptomycin (Gibco, Life Technologies; Grand Island, NY, USA).

Delivered dose

The actual deposited fraction of nanoparticles was modelled according to the method described by (Deloid et al. 2017). For the exposures described above, the mean deposited fraction of silver, titanium dioxide and zinc oxide nanoparticles were 1.2%, 8.1% and 22%, respectively (Poon et al. 2017).

Microarray-based gene expression analyses

200 ng of total RNA from each sample was utilized for gene expression analysis, based on Agilent's Sure Print G3 Human GE v3 8x60K arrays. This platform is designed to target both mRNA and long non-coding transcripts, but for the purpose of simplicity we always refer to microarray transcripts as mRNAs. Raw files were pre-processed (normalization/batch effect removal), followed by differential expression analysis as described previously (Poon et al. 2017). The implemented cut-offs for considering a gene as

significantly different between conditions was a minimum 1.5-fold change in expression at a false discovery rate of at most 5%.

Small RNAseq

An aliquot of the same total RNA used for microarray-based gene expression profiling was used to investigate changes in miRNA expression. Small (15 – 35 bp) RNA-seq libraries for sequencing on Illumina platforms were generated using the SMARTer® smRNA-Seq Kit for Illumina® (Clontech, CA, USA). Library generation, quality control and single-end sequencing on an Illumina NextSeq platform (High Output 75 cycle flow cell, 400M clusters) were performed as a commercial service by the Functional Genomics Unit (FuGU, University of Helsinki).

Identification and quantification of miRNAs/isomiRs

We restricted our analysis to the identification of known miRNAs and their variants. The miRge (Baras et al. 2015) pipeline, dedicated to the identification of novel variants from canonical miRNAs was used. A *fasta* file of all known human miRNAs were obtained from miRbase (version 22, containing 2654 mature human miRNAs). Raw miRNA reads were pre-processed with the *Cutadapt* tool as follows: 5´and 3´ adapter trimming, trim additional 3 bp from 5´ end introduced during SMARTer® PCR, trim 3' ends with > 8bp polyA stretch and finally filter out reads < 16bp. Read alignment and quantification were done in miRge, using default settings (Baras et al. 2015).

Differential expression analysis

The output file of aligned reads – *mapped.csv*, was imported into *Perseus* (Tyanova et al. 2016) omics data analysis platform. All reads that mapped to mRNA, miRNA hairpin and non-miRNA reads were filtered out. All identified unique sequences that were annotated as a miRNA or an isomiR was considered an independently expressed unit, i.e., read counts from highly similar sequences were not combined. Only mapped miRNAs/isomiRs with > 5 counts in at least 3 samples were retained for differential expression (DE) analysis. The cleaned dataset was imported into *Chipster*'s (Kallio et al. 2011) R-based graphical interface for DE analysis. Identification of DE miRNAs between any two exposed versus unexposed group pair was carried using Deseq2 algorithm (Love, Huber, and Anders 2014). DE miRNAs/isomiRs with an adjusted p value < 0.05 were considered significant. In addition, we did not implement any fold change cut-off. Finally, when describing miRNAs/isomiRs, we have used the term miR to refer to either of them.

Hierarchical clustering

Cluster dendrograms were constructed either from normalized (TMM normalization method) non-log transformed count data, using a detrended correspondence analysis approach (implemented in *Chipster*), or from normalized log2-transformed count data using a heatmap (implemented in *Perseus*).

MiRNA/isomiR (miR) target inference and pathway analysis

Interdependencies between THP-1 transcriptome (mRNA/lncRNA) and miRnome (miRNA/isomir) were detected via regularized canonical correlation analysis between the transcriptome and miRnome datasets

using the R-based mixOmics package (Rohart et al. 2017). We implemented a correlation score cut-off of >|0.7| to consider a miRNA-mRNA pair as significantly correlated or anti-correlated. We used the assumption that highly correlated/anti-correlated miRNA/isomiR-mRNA pairs, represented co-regulated and functionally relevant networks. As such, the potential function of these miRNAs/isomiRs was inferred from the enriched biological processes or pathways represented by their correlating/anti-correlating gene (mRNA) pairs. Subsets of significantly correlated mRNA were then submitted to Gene Ontology's Pantherdb (Mi et al. 2017) tool for functional enrichment analysis. A false discovery rate of at most 5% was implemented to consider a pathway as significantly enriched within any subset of highly correlated genes. Correlation-inferred targets were compared to experimentally validated as well as seed sequence-based mRNA targets using Ingenuity's knowledgebase (IPA). In IPA, the targets of closely related sequences (miRNAs and isomiRs) were predicted based on the seed sequences of the canonical miRNA. A third approach to target prediction, was to identify potential mRNA binding sites for unique seed sequences (nucleotides 2 – 8), using the TargetScan database (Agarwal et al. 2015).

Targeted miRNA validation via qPCR

Total RNA (plus miRNAs) was isolated from exposed differentiated THP-1 cells and A549 cells, according to the protocol specifications of Norgen's (Norgen Biotek Corp) Total RNA Purification Plus Kit. 100ng of total RNA were employed for cDNA synthesis using a TaqMan™ MicroRNA Reverse Transcription Kit together with a specific TaqMan™ miRNA Assay RT primer, or TaqMan™ Advanced miRNA cDNA Synthesis Kit (ThermoFisher Scientific). Primers and probes for hsa-miR-6087 (Assay ID: 480183_mir), hsa-miR-142-5p (Assay ID: 477911_mir), hsa-miR-155-3p (Assay ID_477926_mir), hsa-miR-146a-5p (Assay ID: 478399_mir) and RNU48 (small nucleolar RNA SNORD48, Assay ID: 001006), were ordered as pre-designed miRNA assay reagents (ThermoFisher Scientific). Real time amplification was performed with TaqMan's Fast Advanced Master Mix as described in the *TaqMan® miRNA Assays* protocol (Applied Biosystems). Real time amplification was performed in 96-well optical reaction plates on a standard 7500 Fast RT-PCR system (Applied Biosystems). Expression of RNU48 was used as an endogenous control to account for technical variability during sample prep. The relative expression of each miRNA was calculated using the ddCt method.

Data availability

The raw sequencing files, adaptor trimmed *fastq* files or the output file of aligned reads (*mapped.csv*) will be provided by the corresponding author [JN] upon reasonable request.

Results

Expression profile of miRNAs responding to nanoparticle exposure

Total small RNAs isolated from nanoparticle-exposed and control THP-1 cells were sequenced at a depth of 9 to 16 million reads. An average of 160,000 reads per sample were mapped to known miRNA loci (Fig S1A). 4089 unique sequences (miRs) with 5 or more reads in at least three independent exposures were identified (Fig S1B). These were classified as 821 canonical miRNAs and 3268 miRNAs with 5' or 3' sequence variants (isomiRs). Hereinafter, we use miRs to imply both miRNAs and isomiRs. To visualize potential differences between exposure groups as a result of miR transcriptome modulation, we implemented a detrended correspondence analysis on normalized miR counts (Fig 1). A very modest distinction of the different exposures was observed within the first 6 hours. After 24h, the miR transcriptome was drastically modulated by exposure to Ag nanoparticles. TiO_2 nanoparticles also triggered clearly distinct changes on the miR transcriptome, but unlike Ag nanoparticles, the magnitude of the expression change induced by TiO_2 was considerably smaller. When considered separately, the variation in expression was consistent for both canonical miRNAs and isomiRs, but the isomiR profile performed slightly better in distinguishing the 6h exposures from the 24h exposures (Fig S2). Significantly differentially expressed (DE) miRs were identified by comparing the expression levels of miRs identified in exposed samples to that of their corresponding unexposed controls. In total 174 miRs (49 miRNAs and 125 isomiRs) were identified as significantly different (adj. p value < 0.05 and |log2| fold change of 0.23 – 6.85) between exposed and unexposed cells. The list of all significantly DE miRs identified in exposed versus unexposed comparisons are provided in supplementary Table S1. Whilst the majority of DE miRs were triggered in response to TiO_2 nanoparticles ($nTiO_2$: 102, nAg: 80 and nZn: 28) (Fig 2A), the greatest fold changes in miR expression was observed in THP-1 cells exposed to Ag nanoparticles for 24h (Fig 2B). Consistently, a dendrogram of these DE miRs reveal that 24h exposure to silver nanoparticles is the most distinct exposure (Fig 2C). The top DE miRs in the 24h nAg exposures were classified as 2 isomiRs from miR-6797-3p [GGGGGGAGAGAAGGGTCGG (log2 FC, 4.54) and GGGGGGAGAGAAGGGTCG (log2 FC, 4.93)] and 4 canonical miRNAs from miR-6087 [GAGGCGGGGGGGGCGAGC (log2 FC, 6.39), GAGGCGGGGGGGGCGAGCCC (log2 FC, 6.40), GAGGCGGGGGGGCGAG (log2 FC, 6.76) and GAGGCGGGGGGGGCGAGCC (log2 FC, 6.85)]. Only 6% of all DE miRs were common between the three nanoparticles (Fig 2D). 11 isomiRs from miRs -1199-5p, -1260a, -1260b, -5100, -6807-5p, -6872-3p, -6894-3p and -7977, were DE in response to all nanoparticles after 24h, and 2 isomiRs from miR-5100 were DE in response to all 3 nanoparticles within 6h (Fig 2D).

Integrative miR target inference

Predicting miRNA target genes is challenging because a miRNA binds to its target mRNA with partial complementarity over a short (usually nucleotides 2 – 8 from the 5' end) seed sequence, leading to generation of false positive targets. The false-positive rate of sequence-based candidate targets of a given miRNA is thought to be around 30–50% (Alexiou *et al.*, 2009; Watanabe *et al.*, 2007). Furthermore, the seed sequence of isomiRs can be identical to that of their canonical miRNA isoforms, making it

impossible to infer potential alternative targets of these isomiRs. To address this issue, we used an integrative 'omics' approach, wherein microarray-based transcriptomics and smallRNA sequencing data were simultaneously analyzed to identify canonical correlations between mRNA/lncRNA and miRNA/isomiR derived from the same total RNA pool. MiR-mRNA canonical correlation covariates were identified from expression matrices consisting of all 6h and 24h exposures together (Fig 3), and the 6h and 24h exposures separately (Fig S3). In the combined 6h and 24h exposures, 70 miRNAs were identified as positively or negatively correlated (canonical correlation cutoff > 0.7) with 614 mRNAs. A list of these 614 genes is provided as Table S2. Biological process and pathway enrichment analyses was carried out based on these 614 mRNAs. Significant enrichment of processes consistent with cell cycle regulation, inflammatory response and response to metal ions, highlights the potential function and downstream targets of the 70 miRs changing over time and/or in response to nanoparticle exposure. The top enriched pathways are shown in Fig 3. When we performed the canonical correlation analysis separately for the 6h and 24h exposures, we found 33:557 and 203:763 correlated miR-mRNA pairs in the 6h and 24 exposures, respectively. Correlation dendrograms, Venn comparisons and the topmost biological processes represented by unique and overlapping correlated mRNAs are depicted in Fig S3. No significantly enriched biological processes were identified amongst the correlated mRNAs unique to the 6h exposures, while biological processes corresponding to mitotic cell division and chromosomal segregation were prominently enriched by correlating mRNAs unique to the 24h exposures. Biological processes consistent with inflammatory response and response to metal ion were enriched by correlated mRNAs common between the 6h and 24h exposures. Taken together, a canonical correlation analysis of miR and mRNA expression profiles, followed by biological process and pathway enrichment analyses, identified co-regulated miR-mRNA clusters that are functionally implicated in the cellular response of differentiated THP-1 cells to metal-based nanoparticle exposure. The potential of the mRNAs to be downstream targets of their correlated miRNA/isomiR partners is furthermore highlighted by the observation that, a heatmap of either the correlated miRs or mRNAs from the combined 6h and 24h data matrices, clusters all exposures according to time and nanoparticle type, wherein the cells exposed to Ag nanoparticles for 24h are the most distinct exposure at both the miR and mRNA levels (Fig S4).

Correlation-inferred miR-mRNA networks overlap with networks enriched by miR seed sequence-based predicted target genes

As established regulators of gene expression, it can be expected that changes in miR expression occur primarily in response to stimuli, cell division or cellular differentiation. We found that 94% of miRs with a high correlation (>|0.7|) to mRNA expression were DE expressed (ANOVA q value < 0.01) over time, in response to and between exposures (Fig 4A). This is consistent with the previously-mentioned observation that the different exposures and time points are distinguished by hierarchical clustering of these highly correlated miRs (Fig S4). Next, we compared the extent of overlap between correlation-based identification of potential miR target genes and miR sequence-based predicted mRNA targets. Sequence based miR target prediction was carried out using the Ingenuity Knowledgebase (IPA®), which combines information from miRecords, TarBase, TargetScan and Ingenuity Expert Findings to scan a list of input miRNAs for experimentally validated and high predicted mRNA targets. IPA utilizes the miRNA seed sequence (2 to 8 nucleotides from the 5' end) for target prediction. Because the majority of

miRNA variants consists of canonical miRNAs with additional 5'or 3' nucleotides, seed sequences derived from 45 canonical miRNAs could be identified from within the subset of 70 correlated miRs. Of which, 25 were determined to either have experimentally validated or highly predicted mRNA targets (Fig 4B). We filtered out all putative mRNA targets with moderate scores. In total, 3580 target genes were identified, 36 of which had been experimentally validated. Although only 14% of the THP-1 genes with a high correlation to miR expression, were identified from amongst these seed sequence-based predicted target genes (Fig 4C), the top enriched pathways were highly consistent with cellular responses to metal-based nanoparticle exposure (Fig 4D).

A subset of miRs triggered by exposure to Ag nanoparticles, may regulate cellular stress response to different types of metal-based nanoparticles

To further characterize the most relevant DE miRs, we choose DE miRs from the exposures in which most drastic effect on the miR transcriptome had been observed – the 24h Ag nanoparticle exposures. DE miR and mRNA transcripts between 24h nAg-exposed THP-1 cells and their corresponding unexposed controls were selected for further analysis. A Venn comparison was then performed to identify DE miRs and DE mRNAs that overlap with correlated miR-mRNA pairs. Out of the 60 miRs identified as DE in response to 24h Ag nanoparticle exposure, the expression patterns of 7 of them (miR-5100: ATCCCAGCGGGGCCTCC, miR-142-5p: CATAAAGTAGAAAGCACTAC, CCCATAAAGTAGAAAGCACT, miR-6087: GAGGCGGGGGGGCGAGCC, miR-7704: GGGGTCGGCGGCGACG, miR-342-3p: TCTCACACAGAAATCGCACCCGTCT, miR-6894-3p: TGCCCGCATCCTCCACC) were highly correlated to mRNA expression from the same cells (Fig 5A). Meanwhile, 26% (182 genes; Table S3) of the identified DE mRNAs (adj. p value < 0.05) were miR-correlated mRNAs (Fig 5B). The most significant biological process represented by these overlapping mRNA was *stress response to metal ion* (GO:0097501, adj. p value 7E-13). Six of the top 10 biological processes were listed as *cellular response* or *cellular homeostasis* of *zinc*, *copper* and *cadmium ions* (Fig 5C). Within the 24h exposures, the strongest correlations between these potentially co-regulated 7 miRs and 182 genes was observed for Ag and ZnO nanoparticles, with predominantly weak correlations observed between the corresponding transcripts in the titanium dioxide nanoparticle exposures (Fig 5D). When correlated miR-mRNA pairs were compared with DE miRs or DE mRNAs 63 miRs and 432 mRNAs were unique to the correlated miR-mRNA subset (Fig 5A-B; Fig S5A-B). Pathway enrichment analysis on the 432 miR-correlated genes identified cell cycle (GO:000749, adj. p value 3E-29) as the most enriched biological process, with all the other top 10 pathways representing biological processes that correspond to mitotic cell division (Fig S5C). An indication that these 63 miRs and 432 mRNAs are part of a miR-mRNA co-regulated network involved in cell cycle progression. In fact, 9 miRs identified to be DE between 6h- versus 24h-seeded unexposed THP-1 cells, were identified amongst these 63 miRs. 53 miRs and 709 mRNAs were differentially expressed in the nAg-24h vs. Ctrl-24h comparisons, but were not identified as significantly highly correlated (R > 0.7) (Fig 5A-B; Fig S5A-B). That is, these DE miRs and DE mRNAs are very likely not part of a co-regulated network. The topmost biological processes enriched by these 709 mRNA genes corresponded mainly to general cell response to chemical stimulus (Fig S5C).

Because 24h Ag nanoparticle exposure resulted in differential expression of miR-5100, miR-142-5p, miR-142-5p*, miR-6087, miR-7704, miR-342-3p and miR-6894-3p, that were highly correlated (R > 0.8) to genes involved in cellular metal ion response (Fig 5C-D), we next asked whether this regulatory relationship can be indirectly harnessed (expression of these 7 miRNAs) to investigate other types of adverse metal-based exposures. To this end, we compared differentially expressed genes identified from 24h exposures of the same THP-1 cells to nano-sized (20 nm) silver particles, nano-sized (20 nm) zinc oxide particles, bulk-sized (300 nm) zinc oxide particles and non-particulate nitric acid silver ions. Although each exposure type triggered a unique change in the gene expression profile, 10 genes were commonly triggered by both bulk-sized (ZnO) and nano-sized (ZnO and Ag) particles, as well as non-particulate silver ions. While 37 genes were commonly triggered by exposure to the three particles but not silver ion solution (supplementary Figure S6A). Consistently, a *response to metal ion* was identified as the most enriched biological process when GO enrichment analysis was performed based solely on the 10 or 37 common DEGs (supplementary Figure S6B). A list of differentially expressed genes from the 24h exposures is provided as supplementary Table S4.

Upregulation of miR-6087 presented as a distinct hallmark of adverse nAg exposure in THP-1 cells

Canonical and isomeric variants of hsa-miR-6087, were identified as the most upregulated miRs across all exposures. Within 6h of seeding, the average combined expression of reads derived from the miR-6087 locus across all samples was about 552 reads per million mapped reads (RPM). The number of sequenced miR-6087 reads increased to 1,170 RPM in all 24h samples except those exposed to Ag nanoparticles. The average combined expression of miR-6087 miRs in samples exposed to Ag nanoparticles for 24h was starkly contrasting, at 17,774 RPM. A heatmap of normalized and log2 transformed read counts of all identified canonical and variant miRNAs of miR-6087, separates the 24h Ag nanoparticles exposures from all the other exposed and control samples (Fig 6A). When miR-6087 variants with over 100 read counts across all samples are compared to the hsa-miR-6087 stem loop sequence, or aligned against a canonical miR-6087 miRNA (Fig 6B), we find that the majority of these miR-6087 miRNA variants are 3'-isomirs, derived from a combination of both alternative Drosha/Dicer cleavage and RNA editing. 5'-isomiRs of miR-6087 were derived exclusively from alternative Drosha/Dicer cleavage. mRNA target prediction (TargetScanHuman6.0, default settings), based on the alternative seed sequences (nucleotides 2 – 8) generated by the most abundant miR-6087 isomiRs, reveal that only 3% of the potential target genes are shared by 2 or more 5'-isomir variants (Fig 6C).

RT-PCR validation of selected differentially expressed miRs

The expression of 2 (hsa-miR-142-5p and hsa-miR-6087) of the 7 key miRs (see Fig 5A), as well as 2 other miRNAs (hsa-miR-155-3p and hsa-miR-146a-5p) that were available in-house, was validated via qPCR. The expression of these miRs as determined via qPCR was in line with our smallRNAseq data (Fig S7). We could also confirm the upregulation of hsa-miR-6087 and hsa-miR-155-3p in A549 cells exposed to the same concentration of Ag nanoparticles as PMA-differentiated THP-1 cells (Fig S7).

Discussion

In the present study we investigated changes in the expression of miRNAs in response to sub-toxic metal and metal oxide nanoparticles. We also used gene (mRNA) expression profiles from the same cells to predict functional mRNA-miRNA networks linked to early response to metal-based nanoparticles. A variety of RNAseq tools exist, each with certain advantages and limitations, without consensus on an optimal method. We opted for a tool that emphasizes distinction of isomiRs from canonical miRNAs. Being only 19–21 bp long on average, miRNAs/isomiRs will likely align to random sequences. This makes their proper assignment based on alignment to the entirety of the genome difficult and more subject to inaccuracies than mRNAs. To address this issue, we performed alignments against a library consisting of known human miRNA sequences from the miRbase (v22) repository, with 2654 unique mature miRNA entries. Furthermore, because miRNAs can act cooperatively with other miRNAs to modulate gene expression (recently reviewed in Bracken et al. 2016), we chose not to implement any fold change cut-offs during identification of DE miRs. As such, the modestly differentially expressed miRs identified herein should be interpreted with caution. Nonetheless, the identified top correlating miRs, predicted to be involved in cellular response to metal ions were all differentially expressed by more than 1.5-fold.

Recent studies have brought the potential relevance of isomiRs to the forefront by showing that 5' isomiRs are expressed in a cell-specific manner (Neilsen, Goodall, and Bracken 2012), are evolutionary conserved (Tan et al. 2014) and have distinct functions (Yu et al. 2017). In addition to de novo sequence and length variants, the miRge annotation pipeline also distinguishes validated SNPs. As such, the 821 unique miRNA sequences identified were annotated to 215 miRNAs, whilst the 3268 unique isomir sequences were annotated to 540 miRNAs. The most diverse set of miRNA sequence variants identified belonged to all 12 members of the let-7 family of miRNAs – with a total of 97 unique miRNA and 504 unique isomiR sequences. Let-7 miRNAs are the most conserved, and as a result, the most studied miRNA family to date. Whilst there are indications that they may be relevant for normal cellular development, they have also been shown to serve important and functionally redundant roles as tumor suppressors (Su et al. 2012). The occurrence of this pervasive sequence variation in such a highly conserved and physiologically important miRNA family, is in line with recent views that miRNA sequence variation is most likely not an artefact (Desvignes et al. 2015). With all the above in mind, we have favored a quantification and target identification approach that considers each miR (miRNA/isomiR) sequence as a functionally unique miRNA entity.

The observation that the expression profile of all unique miR (miRNA/isomiR) variants distinguished exposure duration and nanoparticle type, echoes conclusions from decades of research that miRNAs are bonafide pathophysiological biomarkers. We are of the opinion that isomiRs can also serve as robust biomarkers. Exposure to TiO_2 and Ag nanoparticles was still observed as the most unique treatments when the expression profile of either the miRNAs or isomiRs were considered separately, although combining miRNA/isomiR profiles better distinguished the time point and exposures than each sub-profile. This suggests that sequence variation is a functionally relevant phenomena that may have evolved as a more efficient way (for example in terms of cell energy resources) to fine tune gene regulation, without the need to increase the total miRNA turnover rate.

The miR-6087 locus was particularly sensitive to nAg exposure. Canonical and length and sequence variants of miR-6087 were drastically upregulated after 24h of exposure to Ag nanoparticles. Further studies are warranted to investigate the functional role of miR-6087 within the context of silver toxicity, and general metal-based nanoparticle toxicity. For now, we can only speculate that, the extensive variation (that potentially modify its mRNA targets), and coordinated upregulation of canonical and variant miR-6087 transcripts may be functionally indispensable for homeostatic immune response to sub-toxic silver exposure.

In terms of number of differentially expressed miRs, it was actually unexpected to find the most in TiO_2-exposed cells because, on the mRNA level, exposure to TiO_2 elicited the least number of differentially genes (Poon et al. 2017). In certain *in vivo* set-ups, TiO_2 nanoparticles have been reported to cause pulmonary toxicity and lung inflammation (reviewed in (Shi et al. 2013)). However, contrary to Ag and ZnO nanoparticles that induce cytotoxicity, inflammation and genotoxicity mostly through dissolution and generation of reactive oxygen species, TiO_2 nanoparticles are in general considered to be stable and insoluble, requiring considerably higher molar concentrations to trigger similar adverse effects like Ag and ZnO nanoparticles. In addition, given that; 76% of the identified DE miRs in TiO_2-exposed cells were downregulated (Fig 2A), 70% of DE miRs in TiO_2-exposed were common between 6h and 24h exposures as opposed to 10% and 15% in nAg- and ZnO-exposed cells, respectively, it seems that the bulk of the identified DE miRNAs/isomiRs in response to TiO_2 nanoparticles can be attributed to miRNA/isomiR binding to the surface of TiO_2. Especially, when also considering that miRNAs/isomiRs with the strongest correlation to a subset of genes related to stress response to metal ion and inflammatory response, were weakly correlated in the TiO_2 exposures. In addition, similar to phosphopeptides, ribonucleotides - the building blocks of miRNAs/isomiRs, have been shown to have a high affinity (over a broad pH range of 2–11) for the surface of TiO_2 (Cleaves et al. 2010). In fact, in the same way that TiO_2-based columns, beads, etc., are being used for adsorption-based enrichment of phosphorylated peptides (Thingholm et al. 2006; Montoya et al. 2011), engineered TiO_2 nanofibers were very recently proposed as a tool for enrichment of miRNAs from biological matrices (Jimenez et al. 2018).

High complementarity between miRNA seed sequence (usually 2 – 8 nucleotides from the 5' end) and mRNA 3' UTRs which results in cleavage through an RNA interference mechanism (Bartel 2004), is the most conserved mechanism of miRNA-mediated gene expression regulation. In contrast, partial complementarity, as may be the case if an isomiR binds the same target as its canonical miRNA or if a canonical miRNA binds 3' UTRs from several genes, results in translational inhibition(Bartel 2009), and is commonly seen in mammalian cells. However, predicting miRNA targets using sequence complementarity-based approaches often leads to false positives and false negatives, because miRNA seed sequence independent features like 5'and 3' length and sequence variants, have been shown to affect target selection and seed-target duplex stability (Hibio et al. 2012). Having access to DE mRNA from the same samples is known to improve seed sequence-based target prediction. Because we considered all identified unique miR sequences as independently expressed units, the integrated miR-mRNA correlation-based target prediction approach we have used treats each sequence variant as a unique variable, thus taking into account the target-modulating potential of length and sequence variants outside the seed region. The biological processes and pathways represented by the mRNA in co-regulated miR-mRNA networks indicate that THP-1 miRNAs/isomiRs regulate the expression of genes involved in cell

cycle regulation, immune response and response to metal ions. This canonical correlation-based approach seems to be highly specific because, firstly, a heatmap based on the identified mRNAs with high correlation (cutoff >|0.7|) to miRNA/isomiR expression, separates all exposures according to duration of exposure and nanoparticle type. Secondly, when we compared the DE genes to miRNA-correlated genes, for example, for the 24h silver nanoparticle exposures (nAg-24h), we find that the top biological processes enriched by the intersecting 182 genes were related to metal ion and inflammatory responses, whilst the 432 DE genes that were unique to the miRNA-correlated subset were more involved in cell cycle related biological processes. These 432 genes may represent genes that are DE between 6h and 24h seeded cells. Finally, 709 genes that were unique to DE genes in nAg-24h, were predominantly involved in response to cytokines. We deduce from this that, in as much as the downstream immune responses (e.g. inflammation) are regulated at the level of the miRNA, the early immune signaling events, like response to cytokine, are regulated in a miRNA-independent manner. The poor dissociation of the different exposures based on 6h miRNA/isomiR expression profiles, supports this view.

Sequences from miRs -142-5p, 142-5p*, -342-3p, -5100, -6087, -6894-3p and -7704 were the most correlated with 182 differentially expressed THP-1 mRNAs that were highly enriched for biological processes corresponding to cellular response to metal (listed as zinc, copper and cadmium in the gene ontology database) ions and inflammatory response. Because the genes responsible for these enriched pathways were triggered in response to Ag nanoparticles, it seems that metal-based nanoparticles have overlapping mechanisms of action. In addition, although we previously (Poon et al. 2017) identified distinct gene expression profiles between THP-1 cells exposed to bulk- vs. nano-sized particles (300 nm ZnO vs. 20 nm ZnO) and between nanoparticles and metal ion solution (nAg vs. Ag+ ion), analysis of shared DEGs revealed *response to metal ion* as a common mechanism of toxicity (Fig S6). Since this pathway is activated (albeit to varying degrees) in response to non-particulate (Ag+), nano-sized (nAg and nZnO) and bulk-sized (bZnO) metal ions, it may constitute a common mechanism of toxicity for a broad class of metal and metal oxide nanoparticles. It follows therefore that, the change in expression of miRNAs identified as potential regulators of its component genes (in this case, the 7 miRs that were highly correlated to metal ion response – Fig 5) may be useful proxies (biomarkers) to investigate adverse exposure to metal-based nanoparticles. Indeed, we find that the degree of correlation within this miR:gene cluster, increases from nTiO_2 to nZnO and nAg exposures (Fig 5D), in very much the same way as the previously assayed cytotoxicity potential of these nanoparticles (Poon et al. 2017). We thus propose that, these 7 DE miRs are components of a co-regulated miR:gene cluster that is triggered in response to metal ions, and changes in their expression may be used to evaluate adverse exposure to metal-based nanoparticles. MiR-6087, miR-7704, miR-5100 and miR-6894-3p were upregulated in nAg-24h, while the two variants of miR-142-5p and miR-342-3p were downregulated in nAg-24h. The fact that we could also confirm the expression of the most upregulated miRNA (miR-6087) in similarly exposed A549 cells (Fig S7), highlights the biomarker potential of this highly correlated miR subset. In reviewing the literature, we find that these miRNAs/isomiRs have been functionally validated in several studies to be involved in processes such as, viral and bacterial immune responses, response to metal ions, cellular differentiation and phagocytosis. For example, Mn^{2+} ion uptake in neuron cells exposed to $MnCl_2$ was shown to trigger upregulation of miR-6087 and miR-7704 (He et al. 2017). Hsa-miR-7704 has also been validated as a miRNA that is upregulated by more than 20-fold in virus-infected dendritic cells

(Baños-Lara et al. 2018). MiR-342-3p was observed to be downregulated in A549 cells exposed to chitosan conjugated gold nanoparticles (Choi et al. 2018). Being a tumor suppressor, downregulation of miR-142-3p has been typically observed in cancer cells (Shen et al. 2013; Xu et al. 2014). Overexpression of miR-142-3p, significantly inhibited E. coli phagocytosis in human monocyte derived macrophages, peripheral blood mononuclear cells, dendritic cells and monocytes (Naqvi, Fordham, and Nares 2015). Implying that downregulation of miR142-3p as observed in THP-1 cells may amplify or promote phagocytosis of nanoparticles.

The above findings, together with the fact that the cells were exposed to particle concentrations that elicited maximum 15% cellular cytotoxicity, support the potential of the miRNAs within the co-regulated miR-mRNA cluster to be biomarkers of early adverse exposure to metal-based nanoparticles.

Conclusion

For most nanoparticles the actual human exposure is unknown, as such, in addition to implementation of minimal human and environmental contact, there has to be biomarkers of early or sub-toxic exposures and rapid identification of hazardous novel nanoparticles. Mechanism-based mode of action approaches for read across, and grouping of nanomaterials based on similar toxicologically relevant features, has been widely adopted by the scientific community as the way forward. Consequently, there has been a steady increase in the volume of experimental data on the mechanisms of biological effects induced by exposure to nanomaterials. However, predictive modelling and classification of related nanoparticles from these data is not straightforward because unlike chemicals, the notion of *dose* when applied to ENM is not only limited to standard particle exposure metrics like mass and concentration. That is, even when assay protocols and test models are harmonized, the determined nanoparticle toxicity constitutes a broad domain of dose-relevant parameters like aggregation state, cellular uptake, solubility, etc., which can be replicated in future studies but are quite challenging to normalize across the bulk of already existing omics datasets. This issue is mitigated by an experimental set-up such as the one from which our data is derived. There-in, exposures were normalized to induce similar levels of the same relevant biological outcome – in this case maximum 15% cellular cytotoxicity. Here-in, we used integrative miRNA/mRNA profiling to propose 7 key miRNAs as possible biomarkers of potentially a broad range of metal-based nanoparticles. In cells exposed for 24h to silver, titanium dioxide or zinc oxide nanoparticles, we showed that the degree of correlation of these miRNAs to differentially expressed metal ion response genes, is proportional to particle cytotoxicity. The rationale of using the expression of these miRNAs to investigate other metal-based nanoparticle exposures, is evidenced by modulation of their potential target genes in response to different types of metal-based nanoparticles and non-particulate metal ions. Of note, none of these 7 miRNAs/isomiRs that were highly predicted to be involved in the regulation of cellular response to metal ions have been identified in the few studies investigating changes in miRNA expression following exposure to Ag, TiO_2 and ZnO nanoparticles (Eom et al. 2014; Huang, Lü, and Ma 2014; Schultz et al. 2016; Zhao et al. 2016). The markedly more elevated nanoparticle mass concentrations employed in those studies may have skewed the identified mechanisms to mostly reflect molecular differences due to biological outcome severity rather than upstream particle-specific bioreactivity – the latter of which, in our opinion, is more relevant to stratify ENM features according to their mode(s) of action. Furthermore, by limiting the extent of cell death most of the identified differentially expressed miRNAs/isomiRs will be biomarkers of early exposure. Ours is the first study that considers both miRNA abundance and canonical miRNA sequence variation, to elucidate sub-toxic, particle-specific immune cell-nanomaterial reactivity.

Disclosure of interest

The authors report no conflict of interest.

References

Agarwal, Vikram, George W. Bell, Jin Wu Nam, and David P. Bartel. 2015. “Predicting Effective MicroRNA Target Sites in Mammalian MRNAs.” *ELife* 4 (AUGUST2015): 1–38.

Baños-Lara, Ma Del Rocio, Jovanny Zabaleta, Jone Garai, Melody Baddoo, and Antonieta Guerrero-Plata. 2018. “Comparative Analysis of MiRNA Profile in Human Dendritic Cells Infected with Respiratory Syncytial Virus and Human Metapneumovirus.” *BMC Research Notes* 11 (1): 1–7.

Baras, Alexander S., Christopher J. Mitchell, Jason R. Myers, Simone Gupta, Lien Chun Weng, John M. Ashton, Toby C. Cornish, Akhilesh Pandey, and Marc K. Halushka. 2015. “MiRge - A Multiplexed Method of Processing Small RNA-Seq Data to Determine MicroRNA Entropy.” *PLoS ONE* 10 (11): 1–16.

Bartel, David P. 2009. “MicroRNAs: Target Recognition and Regulatory Functions.” *Cell* 136 (2): 215–33.

Bartel, David P. 2004. “Review MicroRNAs: Genomics, Biogenesis, Mechanism, and Function Ulation of Hematopoietic Lineage Differentiation in Mam-Mals (Chen et Al., 2004), and Control of Leaf and Flower Development in Plants (Aukerman and Sakai, 2003.” *Cell* 116: 281–97.

Bracken, Cameron P., Hamish S. Scott, and Gregory J. Goodall. 2016. “A Network-Biology Perspective of MicroRNA Function and Dysfunction in Cancer.” *Nature Reviews Genetics* 17 (12): 719–32. https://doi.org/10.1038/nrg.2016.134.

Choi, Seon Young, Pan Dong Ryu, Sang-Woo Joo, and So Yeong Lee. 2018. “Alteration of MicroRNA Expression Profiles by Surface-Modified Gold Nanoparticles in Human Lung Adenocarcinoma Cells.” *Journal of Nanoscience and Nanotechnology* 18 (4): 3024–30.

Cleaves, H James, Caroline M Jonsson, Christopher L Jonsson, Dimitri A Sverjensky, and Robert M Hazen. 2010. “Adsorption of Nucleic Acid Components on Rutile (TiO2) Surfaces.” *Astrobiology* 10 (3): 311–23.

Contado, Catia. 2015. “Nanomaterials in Consumer Products: A Challenging Analytical Problem.” *Frontiers in Chemistry* 3 (August): 48.

Deloid, Glen M., Joel M. Cohen, Georgios Pyrgiotakis, and Philip Demokritou. 2017. “Preparation, Characterization, and in Vitro Dosimetry of Dispersed, Engineered Nanomaterials.” *Nature Protocols* 12 (2): 355–71.

Desvignes, T., P. Batzel, E. Berezikov, K. Eilbeck, J. T. Eppig, M. S. McAndrews, A. Singer, and J. H. Postlethwait. 2015. “MiRNA Nomenclature: A View Incorporating Genetic Origins, Biosynthetic Pathways, and Sequence Variants.” *Trends in Genetics* 31 (11): 613–26.

Eom, Hyun Jeong, Nivedita Chatterjee, Jeongsoo Lee, and Jinhee Choi. 2014. “Integrated MRNA and Micro RNA Profiling Reveals Epigenetic Mechanism of Differential Sensitivity of Jurkat T Cells to AgNPs and Ag Ions.” *Toxicology Letters* 229 (1): 311–18.

Fadeel, Bengt, Lucian Farcal, Barry Hardy, Socorro Vázquez-Campos, Danail Hristozov, Antonio Marcomini, Iseult Lynch, Eugenia Valsami-Jones, Harri Alenius, and Kai Savolainen. 2018. “Advanced Tools for the Safety Assessment of Nanomaterials.” *Nature Nanotechnology* 13 (7):

537–43.

Gebert, Luca F.R., and Ian J. MacRae. 2018. “Regulation of MicroRNA Function in Animals.” *Nature Reviews Molecular Cell Biology* 20 (January).

He, Rong, Xiaoyun Xie, Linyue Lv, Yongqi Huang, Xianmin Xia, Xiaowu Chen, and Lei Zhang. 2017. “Comprehensive Investigation of Aberrant MicroRNAs Expression in Cells Culture Model of MnCl2-Induced Neurodegenerative Disease.” *Biochemical and Biophysical Research Communications* 486 (2): 342–48.

Hibio, Naoki, Kimihiro Hino, Eigo Shimizu, Yoshiro Nagata, and Kumiko Ui-Tei. 2012. “Stability of MiRNA 5′terminal and Seed Regions Is Correlated with Experimentally Observed MiRNA-Mediated Silencing Efficacy.” *Scientific Reports* 2: 21–26.

Hristozov, Danail, Stefania Gottardo, Elena Semenzin, Agnes Oomen, Peter Bos, Willie Peijnenburg, Martie van Tongeren, et al. 2016. “Frameworks and Tools for Risk Assessment of Manufactured Nanomaterials.” *Environment International* 95: 36–53.

Hristozov, Danail R., Stefania Gottardo, Andrea Critto, and Antonio Marcomini. 2012. “Risk Assessment of Engineered Nanomaterials: A Review of Available Data and Approaches from a Regulatory Perspective.” *Nanotoxicology* 6 (March 2011): 1–19.

Huang, Yan, Xiaoying Lü, and Jingwu Ma. 2014. “Toxicity of Silver Nanoparticles to Human Dermal Fibroblasts on MicroRNA Level.” *Journal of Biomedical Nanotechnology* 10 (11): 3304–17.

Jimenez, Luis A, Marissa A Gionet-Gonzales, Sabrina Sedano, Jocelyn G Carballo, Yomara Mendez, and Wenwan Zhong. 2018. “Extraction of MicroRNAs from Biological Matrices with Titanium Dioxide Nanofibers.” *Analytical and Bioanalytical Chemistry* 410 (3): 1053–60.

Kallio, M. Aleksi, Jarno T. Tuimala, Taavi Hupponen, Petri Klemelä, Massimiliano Gentile, Ilari Scheinin, Mikko Koski, Janne Käki, and Eija I. Korpelainen. 2011. “Chipster: User-Friendly Analysis Software for Microarray and Other High-Throughput Data.” *BMC Genomics* 12.

Love, Michael I., Wolfgang Huber, and Simon Anders. 2014. “Moderated Estimation of Fold Change and Dispersion for RNA-Seq Data with DESeq2.” *Genome Biology* 15 (12): 1–21.

Mi, Huaiyu, Xiaosong Huang, Anushya Muruganujan, Haiming Tang, Caitlin Mills, Diane Kang, and Paul D. Thomas. 2017. “PANTHER Version 11: Expanded Annotation Data from Gene Ontology and Reactome Pathways, and Data Analysis Tool Enhancements.” *Nucleic Acids Research* 45 (D1): D183–89.

Montoya, Alex, Luisa Beltran, Pedro Casado, Juan Carlos Rodríguez-Prados, and Pedro R. Cutillas. 2011. “Characterization of a TiO2 Enrichment Method for Label-Free Quantitative Phosphoproteomics.” *Methods* 54 (4): 370–78.

Naqvi, Afsar Raza, Jezrom B. Fordham, and Salvador Nares. 2015. “MiR-24, MiR-30b, and MiR-142-3p Regulate Phagocytosis in Myeloid Inflammatory Cells.” *The Journal of Immunology* 194 (4): 1916–27.

Neilsen, Corine T., Gregory J. Goodall, and Cameron P. Bracken. 2012. “IsomiRs - The Overlooked Repertoire in the Dynamic MicroRNAome.” *Trends in Genetics* 28 (11): 544–49.

Piccinno, Fabiano, Fadri Gottschalk, Stefan Seeger, and Bernd Nowack. 2012. “Industrial Production Quantities and Uses of Ten Engineered Nanomaterials in Europe and the World.” *Journal of Nanoparticle Research* 14 (9).

Poon, W.-L., H. Alenius, J. Ndika, V. Fortino, V. Kolhinen, A. Meščeriakovas, M. Wang, et al. 2017. “Nano-Sized Zinc Oxide and Silver, but Not Titanium Dioxide, Induce Innate and Adaptive Immunity and Antiviral Response in Differentiated THP-1 Cells.” *Nanotoxicology* 11 (7).

Rohart, Florian, Benoît Gautier, Amrit Singh, and Kim Anh Lê Cao. 2017. “MixOmics: An R Package for ‘omics Feature Selection and Multiple Data Integration.” *PLoS Computational Biology* 13 (11): 1–19.

Schultz, Carolin L., Anye Wamucho, Olga V. Tsyusko, Jason M. Unrine, Alison Crossley, Claus Svendsen, and David J. Spurgeon. 2016. “Multigenerational Exposure to Silver Ions and Silver Nanoparticles Reveals Heightened Sensitivity and Epigenetic Memory in Caenorhabditis Elegans.” *Proceedings of the Royal Society B: Biological Sciences* 283 (1832).

Shen, Wei Wei, Zhi Zeng, Wen Xia Zhu, and Guo Hui Fu. 2013. “MiR-142-3p Functions as a Tumor Suppressor by Targeting CD133, ABCG2, and Lgr5 in Colon Cancer Cells.” *Journal of Molecular Medicine* 91 (8): 989–1000.

Shi, Hongbo, Ruth Magaye, Vincent Castranova, and Jinshun Zhao. 2013. “Titanium Dioxide Nanoparticles: A Review of Current Toxicological Data.” *Particle and Fibre Toxicology* 10 (April): 15.

Shyamasundar, Sukanya, Cheng Teng Ng, Lin Yue Lanry Yung, Shaikali Thameem Dheen, and Boon Huat Bay. 2015. “Epigenetic Mechanisms in Nanomaterial-Induced Toxicity.” *Epigenomics* 7 (3): 395–411.

Stokowy, Tomasz, Markus Eszlinger, Michał Świerniak, Krzysztof Fujarewicz, Barbara Jarząb, Ralf Paschke, and Knut Krohn. 2014. “Analysis Options for High-Throughput Sequencing in MiRNA Expression Profiling.” *BMC Research Notes* 7 (1).

Su, Jen-Liang, Pai-Sheng Chen, Gunnar Johansson, and Min-Liang Kuo. 2012. “Function and Regulation of Let-7 Family MicroRNAs.” *MicroRNA E* 1 (1): 34–39.

Tan, Geok Chin, Elcie Chan, Attila Molnar, Rupa Sarkar, Diana Alexieva, Ihsan Mad Isa, Sophie Robinson, et al. 2014. “5′ IsomiR Variation Is of Functional and Evolutionary Importance.” *Nucleic Acids Research* 42 (14): 9424–35.

Thingholm, Tine E, Thomas J D Jørgensen, Ole N Jensen, and Martin R Larsen. 2006. “Highly Selective Enrichment of Phosphorylated Peptides Using Titanium Dioxide.” *Nature Protocols* 1 (November): 1929.

Tyanova, Stefka, Tikira Temu, Pavel Sinitcyn, Arthur Carlson, Marco Y. Hein, Tamar Geiger, Matthias Mann, and Jürgen Cox. 2016. “The Perseus Computational Platform for Comprehensive Analysis of (Prote)Omics Data.” *Nature Methods* 13 (9): 731–40.

Wong, Belinda Shu Ee, Qidong Hu, and Gyeong Hun Baeg. 2017. “Epigenetic Modulations in Nanoparticle-Mediated Toxicity.” *Food and Chemical Toxicology* 109: 746–52.

Xu, Guoxing, Jin Wang, Yixin Jia, Feng Shen, Wensheng Han, and Yifan Kang. 2014. “MiR-142-3p

Functions as a Potential Tumor Suppressor in Human Osteosarcoma by Targeting HMGA1." *Cellular Physiology and Biochemistry* 33 (5): 1329–39.

Yu, Feng, Katherine A. Pillman, Corine T. Neilsen, John Toubia, David M. Lawrence, Anna Tsykin, Michael P. Gantier, David F. Callen, Gregory J. Goodall, and Cameron P. Bracken. 2017. "Naturally Existing Isoforms of MiR-222 Have Distinct Functions." *Nucleic Acids Research* 45 (19): 11371–85.

Zhao, Yong, Lan Li, Ling-Jiang Min, Lian-Qin Zhu, Qing-Yuan Sun, Hong-Fu Zhang, Xin-Qi Liu, et al. 2016. "Regulation of MicroRNAs, and the Correlations of MicroRNAs and Their Targeted Genes by Zinc Oxide Nanoparticles in Ovarian Granulosa Cells." *PLOS ONE* 11 (5): e0155865.

Table 1: Particle characteristics provided by manufacturer

Nanoparticle	**Ag**	**TiO_2**	**ZnO**
Coating	Polyvinylpyrrolidone	-	-
Dissolution	1 ppb – 2 ppm/H_2O	supplied as powder	supplied as powder
Phase	-	90:10(anatase:rutile)	-
Purity (%)	99.99	99.00	99.50
Size (nm)	20	30-40	20
Specific surface area (m^2/g)	27.4	30	50
[#]Hydrodynamic size (nm) in cRPMI	86.43±0.77	642.00±18.04	377.80±5.33
[#]Zeta potential value (mV) in cRPMI	-10.60±1.19	-10.90±0.59	-11.50±1.01

[#]Poon et al. 2017

Figures

Figure 1

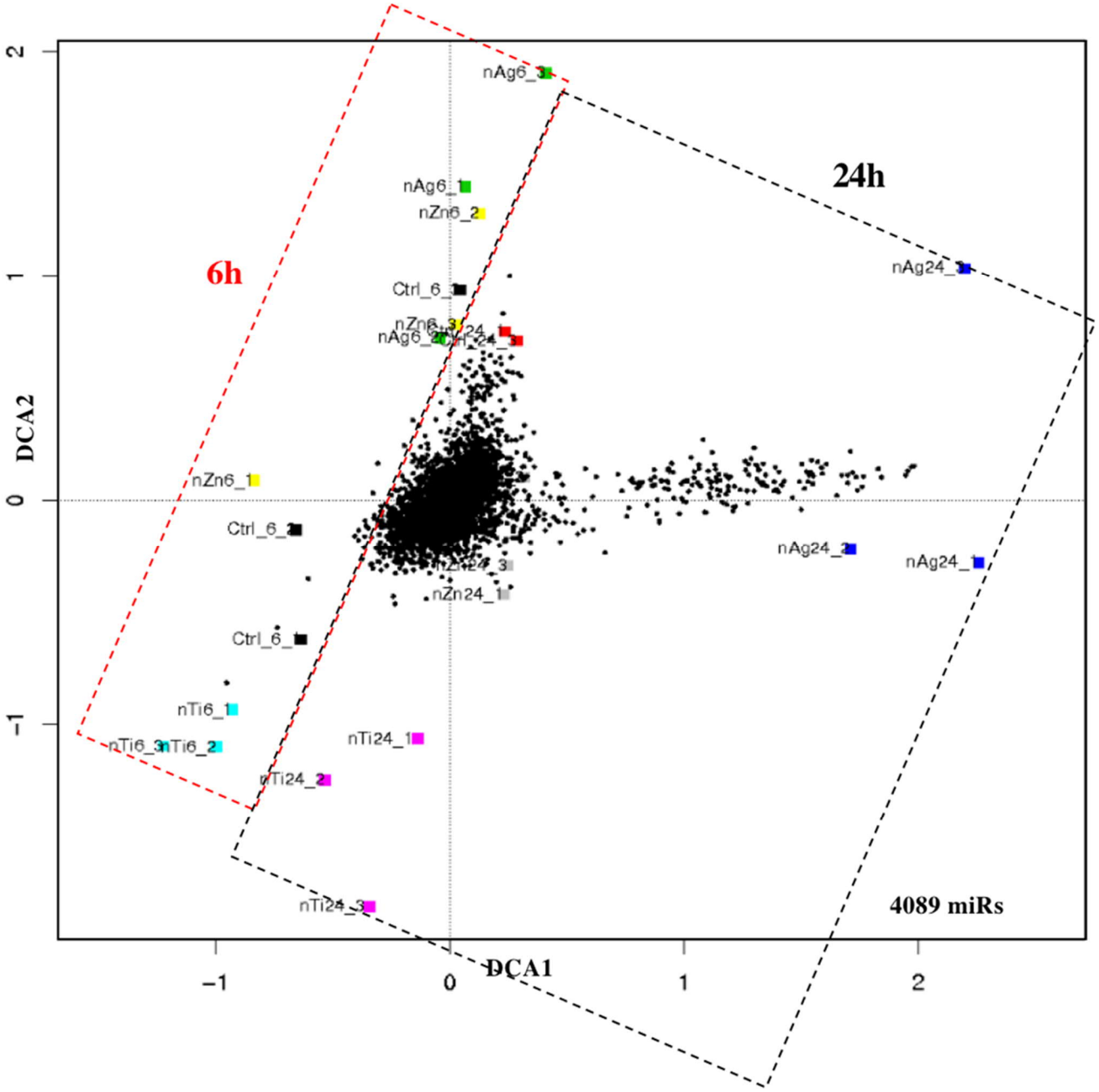

Expression profile overview of miR (miRNA/isomiR) transcripts. Detrended correspondence analysis of global miR expression reveal relatively minor change in expression within 6h as opposed to 24h. Silver nanoparticles (nAg) induced drastic (the biggest) changes in miR expression, after 24 hours of exposure. The dotted red square includes all samples (coloured symbols) exposed for 6h and the dotted black square all the samples exposed to nanoparticles for 24h.

Figure 2

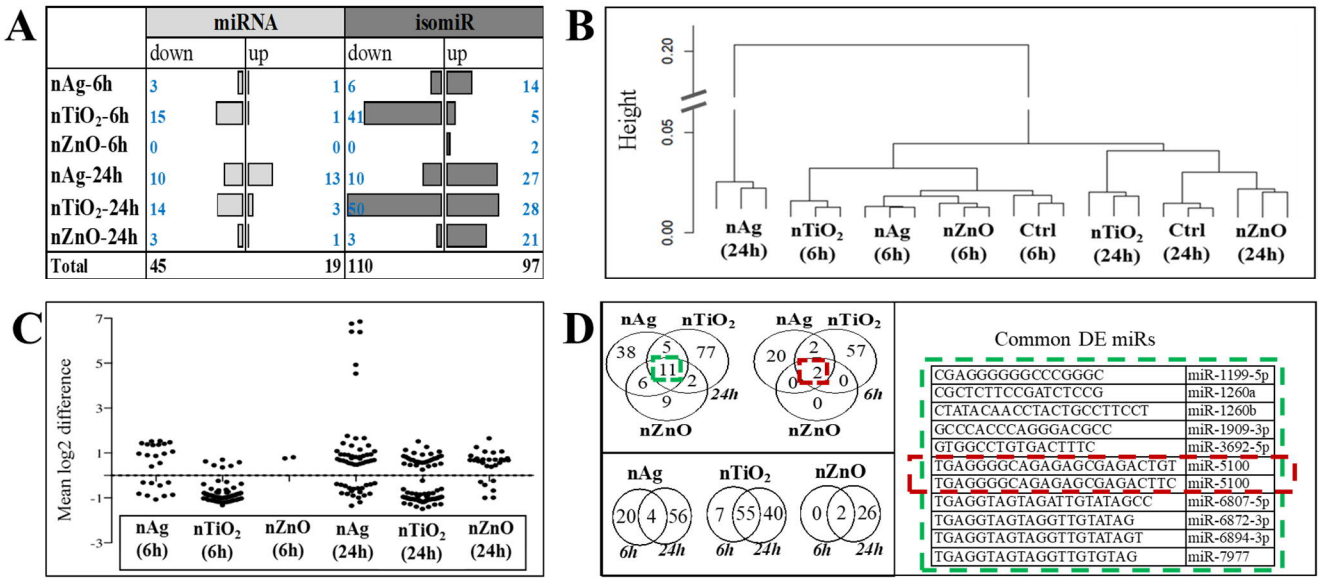

Differentially expressed (DE) miRs between exposed and unexposed controls. Transcriptome of exposed versus unexposed cells were analysed for DE of unique miR sequences (**A**). The length of the bars represents the number of downregulated or upregulated miRs. The exposure with the most severe effect on the miR transcriptome was identified by constructing a cluster dendrogram based solely on DE genes between exposed and unexposed control cells (**B**). 24 hours (24h) exposure to silver nanoparticles (nAg) induced the most drastic change on the miR transcriptome. This is in line with the identification of the most DE miRs in cells exposed to nanosilver for 24h (**C**). DE miRs were compared across nanoparticles with the same exposure duration. Venn comparisons of DE expressed miRs, at each time point across all nanoparticles, or for each nanoparticle across time points are shown in (**D**). The miRs that were commonly DE across the different nanoparticle exposures were classified as isomiRs. Their sequences and names are outlined next to the Venn comparisons.

Figure 3

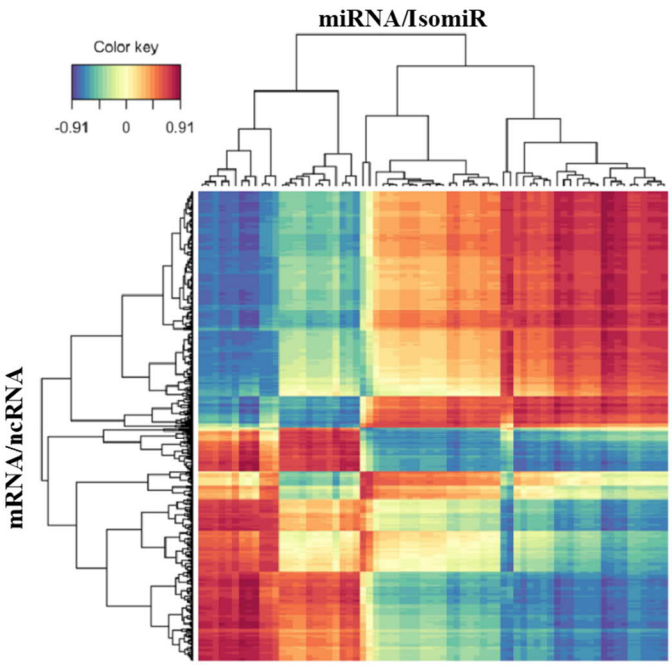

Enriched functions

GO biological process	FDR
mitotic cell cycle process (GO:1903047)	3,E-09
response to stress (GO:0006950)	2,E-07
cell division (GO:0051301)	2,E-07
response to inorganic substance (GO:0010035)	1,E-05
response to lipopolysaccharide (GO:0032496)	1,E-05
inflammatory response (GO:0006954)	2,E-05
regulation of cell cycle (GO:0051726)	2,E-05
response to molecule of bacterial origin (GO:0002237)	3,E-05
regulation of mitotic cell cycle (GO:0007346)	4,E-05
mitotic cell cycle phase transition (GO:0044772)	4,E-05
cell cycle phase transition (GO:0044770)	4,E-05
response to zinc ion (GO:0010043)	4,E-05

Reactome pathways	FDR
Cell Cycle, Mitotic (R-HSA-69278)	2,E-08
Cell Cycle (R-HSA-1640170)	3,E-08
Mitotic Prometaphase (R-HSA-68877)	3,E-04
Metallothioneins bind metals (R-HSA-5661231)	3,E-04
Response to metal ions (R-HSA-5660526)	4,E-04
Resolution of Sister Chromatid Cohesion (R-HSA-2500257)	6,E-04
M Phase (R-HSA-68886)	2,E-03
Separation of Sister Chromatids (R-HSA-2467813)	2,E-02
Mitotic G2-G2/M phases (R-HSA-453274)	2,E-02
Mitotic Metaphase and Anaphase (R-HSA-2555396)	2,E-02

miR target gene and functional effect prediction. In order to identify the genes that are potentially modulated by the identified miRs, a correlation analysis between miR expression and microarray-derived mRNA expression on RNA obtained from the same cells was performed. The heatmap (left panel) shows significant negative and positive correlations (cutoff > 0.7) between the mRNA/lncRNA and miRNA/isomiR data layers. Pathways enriched by these top correlating genes are shown in the right panel.

Figure 4

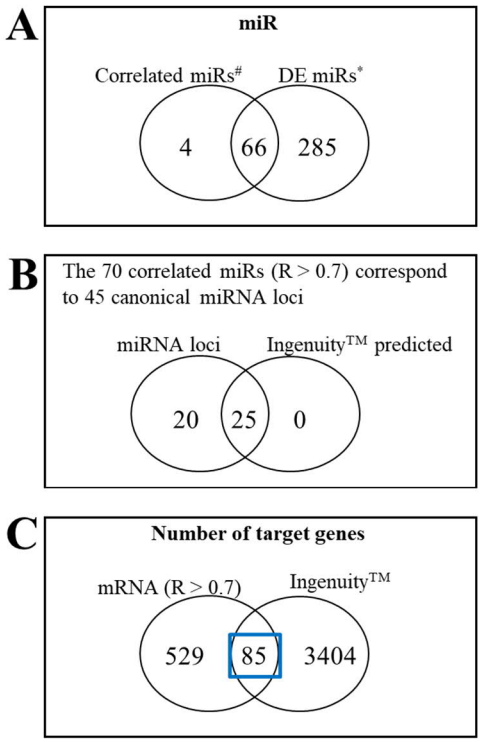

D

GO biological process complete	Fold Enrichment	FDR
stress response to copper ion (GO:1990169)	61.2	2.7E-03
detoxification of copper ion (GO:0010273)	61.2	3.1E-03
negative regulation of lipopolysaccharide-mediated signaling pathway (GO:0031665)	61.2	1.1E-02
detoxification of inorganic compound (GO:0061687)	57.6	2.9E-03
stress response to metal ion (GO:0097501)	54.4	2.8E-03
cellular response to zinc ion (GO:0071294)	40.8	4.8E-03
cellular response to copper ion (GO:0071280)	35.0	6.3E-03
T cell migration (GO:0072678)	30.6	4.3E-02
cellular zinc ion homeostasis (GO:0006882)	29.7	6.9E-03
regulation of lipopolysaccharide-mediated signaling pathway (GO:0031664)	29.4	4.5E-02
response to copper ion (GO:0046688)	27.8	2.9E-03
zinc ion homeostasis (GO:0055069)	27.2	9.2E-03
cellular response to cadmium ion (GO:0071276)	25.8	1.0E-02
response to zinc ion (GO:0010043)	21.9	4.6E-03
skeletal muscle cell differentiation (GO:0035914)	18.5	2.4E-02
intrinsic apoptotic signaling pathway in response to DNA damage (GO:0008630)	17.7	6.3E-03
response to cadmium ion (GO:0046686)	15.1	4.3E-02
cellular transition metal ion homeostasis (GO:0046916)	11.1	2.8E-02
detoxification (GO:0098754)	10.6	3.3E-02
intrinsic apoptotic signaling pathway (GO:0097193)	9.7	1.6E-02
apoptotic signaling pathway (GO:0097190)	7.0	9.7E-03
inflammatory response (GO:0006954)	5.6	4.8E-03
negative regulation of protein phosphorylation (GO:0001933)	5.0	4.9E-02
regulation of protein serine/threonine kinase activity (GO:0071900)	4.9	1.5E-02
response to toxic substance (GO:0009636)	4.5	4.6E-02

#miRs with high correlation (R > 0.7) to mRNA
*miRs that were differentially expressed between all groups (ANOVA q value < 0.01)

Comparison of correlation-based and sequence-based target prediction. Venn comparison between miRs (**A**) identified to have a high correlation (cutoff, R >|0.7|) with mRNA expression and those identified as differentially expressed across time points and exposures (ANOVA q value < 0.01). 45 canonical seed sequences (nucleotides 2 – 8) of most frequently observed miRNA) could be identified from the set of 70 mRNA-correlated miRs. Experimentally validated or high predicted target genes were identified via IPA® miRNA target filtering, for 55% of the submitted canonical miRNAs (**B**). 85 targets of the canonical miRNAs were identified to be amongst the miR:mRNA highly correlating transcript pairs (**C**). The topmost biological processes enriched by these 85 genes are depicted in (**D**). FDR is the false discovery rate.

Figure 5

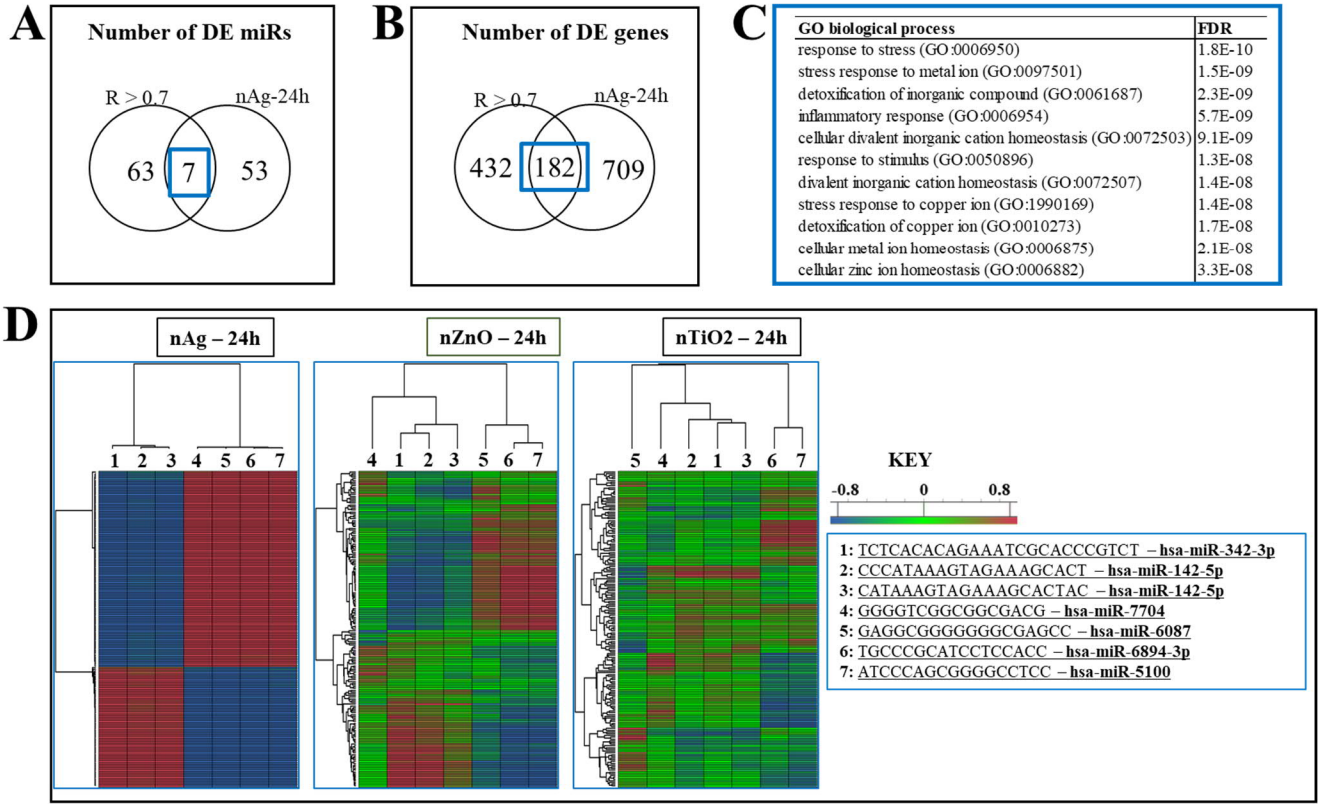

Correlated miR: mRNA pairs relevant to silver nanoparticle exposure. To identify exposure-related genes that were potentially modulated via miRNA targeting, the miRs (miRNA/isomiR) (**A**) and genes (**B**) identified as differentially expressed (*Benjamini-Hochberg* FDR < 0.05, log2 difference > 0.58) in cells exposed to silver nanoparticles for 24h were compared with the correlated miR-mRNA pairs identified via canonical correlation analysis of mRNA and miRs from all exposed and control cells. Venn comparisons reveal 7 miRs and 182 genes are potentially co-regulated in response to silver nanoparticle exposure. These 182 genes consisted of significantly enriched subsets of genes involved in cellular responses to metal ion (**C**). Within the 24h exposures, the strongest correlations between these potentially co-regulated cluster of 7 miRs and 182 genes was observed for silver nanoparticles (nAg) followed by zinc oxide nanoparticles (nZnO), and predominantly weak correlations in titanium dioxide nanoparticle ($nTiO_2$) exposures (**D**).

Figure 6

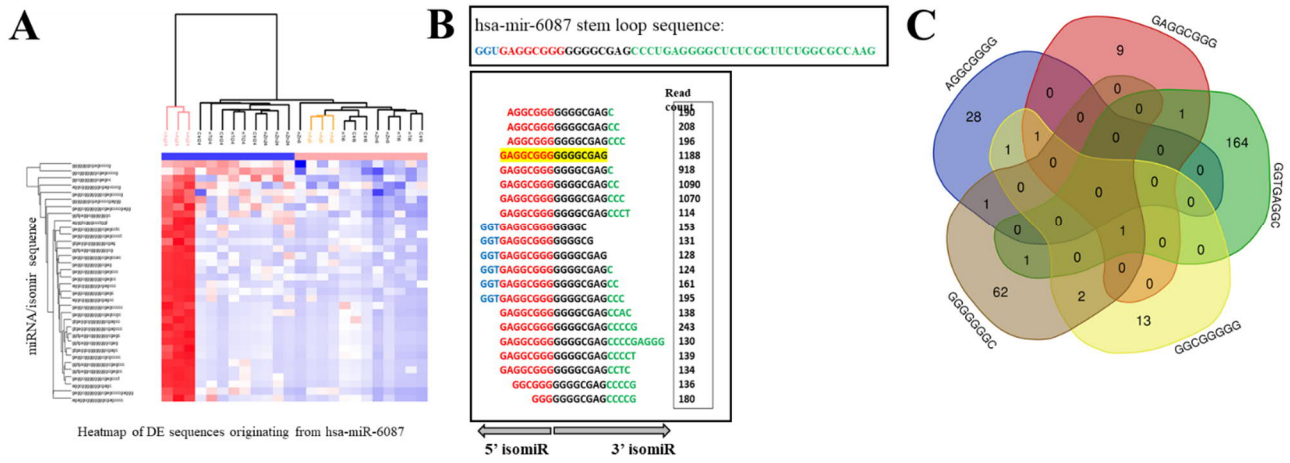

Functional relevance of miR sequence variants. miR-6087 was the most upregulated miR across all nanoparticle exposures. Several canonical and isomeric variants of miR-6087 were upregulated in the 24h silver nanoparticle exposures. A heatmap of all identified miR-6087 transcripts is depicted in (**A**). In (**B**), sequence alignment of the most abundant variants (> 100 read counts across all samples) relative to a canonical mir-6087 miRNA sequence (highlighted in yellow) is shown. Red characters represent the canonical seed sequence, blue characters – 5' sequence variants (5'-isomiR) and green characters – 3' sequence variants (3'-isomiR). Potential differential mRNA targeting, as a result of variations in the seed sequence of miR-6087 are shown as Venn comparisons in (C). Sequence-based miR target prediction was done via TargetScan, using default settings.

Supplementary files

Figure S1: **Read count distribution.** Total (A) and unique (B) read counts are shown for each biological replicate. On average, 150,000 reads corresponding to approximately 1700 to 2900 unique miRNAs with a minimum of 5 read counts, were identified across all samples.

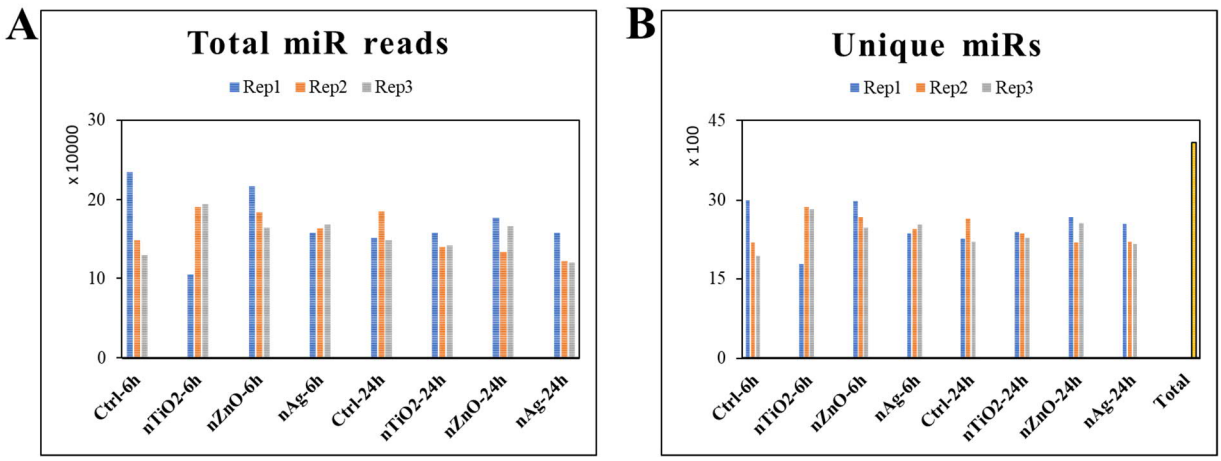

Figure S2: Side by side comparison of canonical and variant miRNA expression reveal consistent response to nanoparticles. A slightly better distinction of exposure duration was observed for the variant containing miRNAs (isomiRs). The dotted red square includes all samples (coloured symbols) exposed for 6h and the dotted black square all the samples exposed to nanoparticles for 24h.

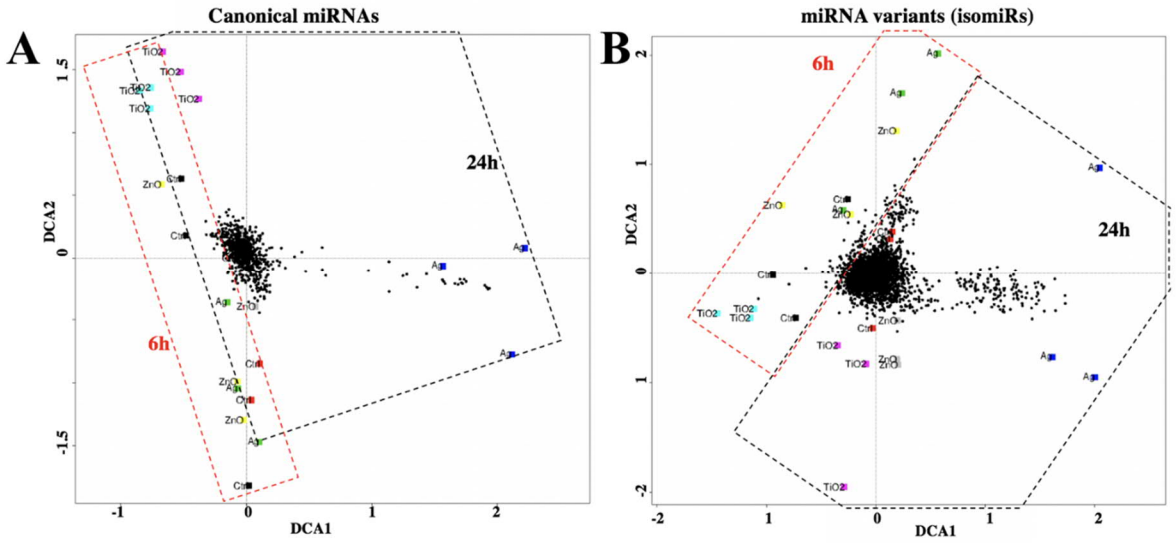

Figure S3: **Integrative miR:mRNA transcriptome correlation-based miRNA target prediction.** (**A**) Heatmap of correlated (cutoff >|0.7|) miR:gene pairs, for 6 hours and 24 hours exposures. (**B**) Venn comparisons of correlated miRs and genes between time points. (**C**) Biological processes enriched by correlated genes that were common to 6h and 24 exposures (red box), unique to 24h exposures (blue box) or unique to 6h exposures (black box).

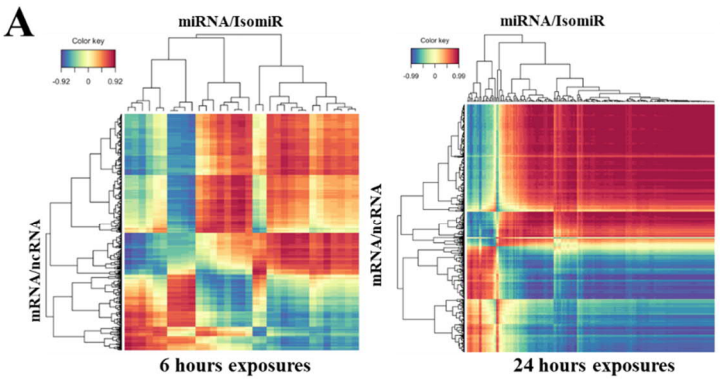

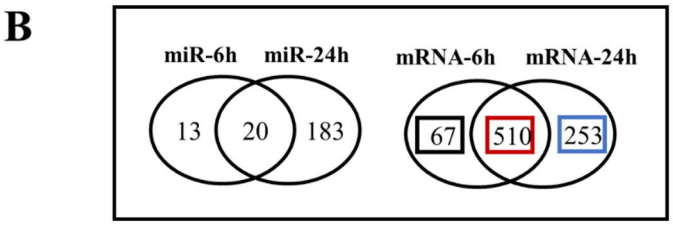

C

GO biological process	Reference	Dataset	FDR
response to stress (GO:0006950)	3412	155	7.93E-17
inflammatory response (GO:0006954)	477	42	4.02E-10
response to stimulus (GO:0050896)	8293	254	6.14E-10
stress response to metal ion (GO:0097501)	18	12	1.31E-09
response to cadmium ion (GO:0046686)	65	17	2.60E-09
regulation of molecular function (GO:0065009)	3222	127	7.78E-09
detoxification of inorganic compound (GO:0061687)	17	11	9.37E-09
cellular response to chemical stimulus (GO:0070887)	2760	113	1.26E-08
apoptotic process (GO:0006915)	905	55	1.48E-08
detoxification (GO:0098754)	115	19	5.29E-08
response to chemical (GO:0042221)	4331	152	5.35E-08
stress response to copper ion (GO:1990169)	16	10	5.45E-08

GO biological process	Reference	Dataset	FDR
cell cycle (GO:0007049)	1314	60	8.68E-18
cell cycle process (GO:0022402)	955	48	3.38E-15
mitotic cell cycle (GO:0000278)	673	39	5.12E-14
nuclear division (GO:0000280)	275	27	5.64E-14
cell division (GO:0051301)	486	34	6.22E-14
mitotic cell cycle process (GO:1903047)	576	36	9.16E-14
chromosome segregation (GO:0007059)	263	26	1.14E-13
organelle fission (GO:0048285)	301	27	2.29E-13
nuclear chromosome segregation (GO:0098813)	214	23	1.18E-12
regulation of mitotic nuclear division (GO:0007088)	185	19	8.27E-10
chromosome organization (GO:0051276)	1030	40	2.69E-09
regulation of cell cycle (GO:0051726)	1137	42	3.03E-09

GO biological process	Reference	Dataset	FDR
regulation of cell differentiation (GO:0045595)	1733	17	7.67E-02
tube development (GO:0035295)	832	10	2.40E-01
sex differentiation (GO:0007548)	265	6	2.71E-01
positive regulation of vitamin metabolic process (GO:	4	2	3.13E-01
regulation of developmental process (GO:0050793)	2486	19	3.23E-01
epithelial cell proliferation (GO:0050673)	83	4	3.51E-01
tube morphogenesis (GO:0035239)	643	9	3.52E-01
cytokine production (GO:0001816)	150	5	4.20E-01

Figure S4: **Side by side heatmaps of correlated miRs** (left) and genes (right). MiR and mRNA transcriptome were profiled in same total RNA pool obtained from unexposed (Ctrl) THP-1 cells or THP-1 cells exposed to titanium dioxide (nTi), zinc oxide (nZn) and silver (nAg) nanoparticles, for 6h or 24h.

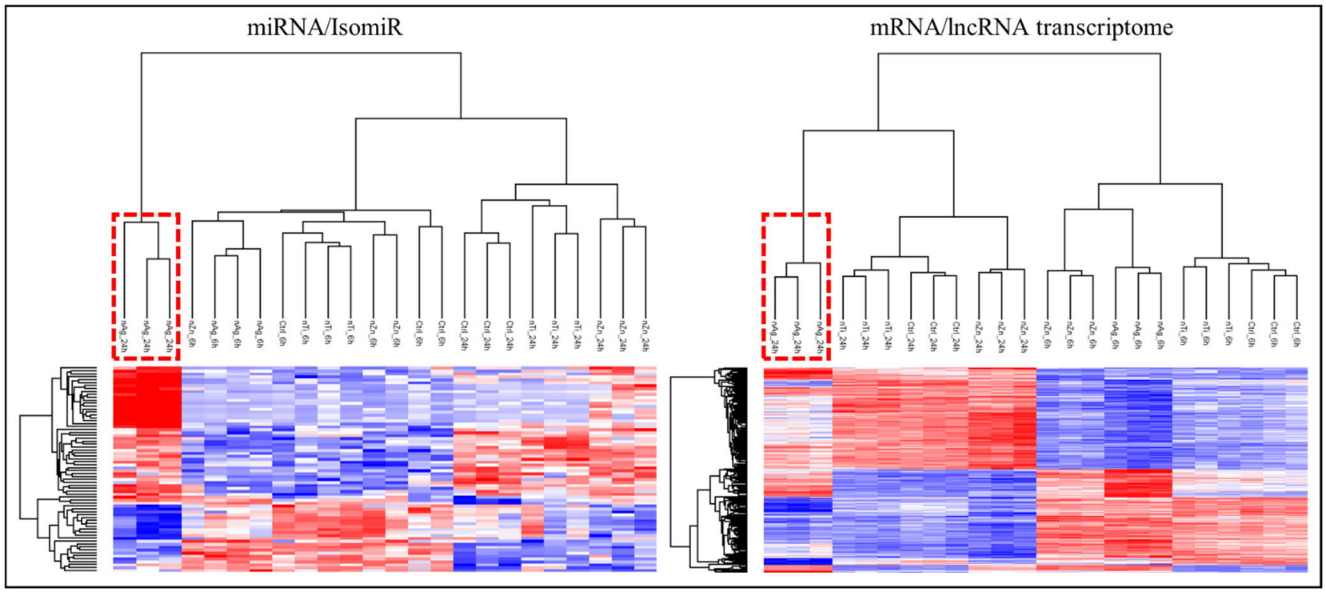

Figure S5: Venn comparison between miRs (**A**) identified to have a high correlation (cutoff >|0.7|) with mRNA expression and those identified as differentially expressed following 24h exposure to silver nanoparticles (nAg). Similarly, mRNAs that correlated with miR expression (cutoff >|0.7|) were compared to those that were differentially expressed as a result of 24h exposure to silver nanoparticles (**B**). The topmost enriched biological processes, represented by the unique mRNAs from the set of compared mRNAs in (B), are depicted in (**C**) and (**D**). FDR is the false discovery rate.

A

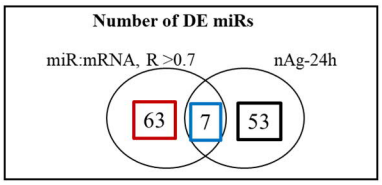

B

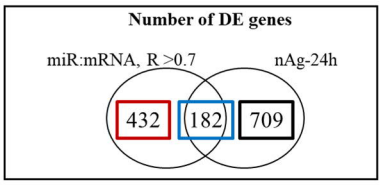

C

GO biological process	FDR
cell cycle (GO:0007049)	3.E-29
cell cycle process (GO:0022402)	2.E-26
mitotic cell cycle process (GO:1903047)	2.E-25
mitotic cell cycle (GO:0000278)	4.E-25
cell division (GO:0051301)	2.E-21
chromosome segregation (GO:0007059)	3.E-18
nuclear division (GO:0000280)	2.E-17
organelle fission (GO:0048285)	3.E-16
regulation of mitotic cell cycle (GO:0007346)	2.E-15
nuclear chromosome segregation (GO:0098813)	2.E-15

D

GO biological process	FDR
response to stimulus (GO:0050896)	7.E-20
cellular response to chemical stimulus (GO:0070887)	3.E-17
response to organic substance (GO:0010033)	1.E-15
response to external stimulus (GO:0009605)	4.E-14
cellular response to stimulus (GO:0051716)	7.E-14
response to chemical (GO:0042221)	1.E-13
cell communication (GO:0007154)	1.E-13
signaling (GO:0023052)	1.E-12
cellular response to organic substance (GO:0071310)	6.E-12
regulation of multicellular organismal process (GO:0051239)	7.E-12

Figure S6: Venn comparison of differentially expressed genes (*Benjamini-Hochberg* FDR < 0.05, log 2 difference > 0.58) in cells exposed to bulk-sized ZnO particles (bZnO – 300 nm), nano-sized ZnO particles (nZnO – 20 nm), Ag nanoparticles (nAg – 20 nm) and non-particulate nitric acid silver [Ag (1+)] is shown in (**A**). Response to metal (zinc, copper, cadmium) ion is the most enriched pathway represented by shared (10 genes in all exposures and 37 genes particle-based exposures) differentially expressed genes (**B**). Metal ion response related pathways are highlighted in green.

A

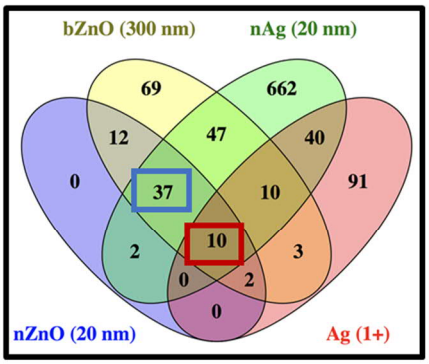

B

GO biological process	FDR
stress response to metal ion (GO:0097501)	5.09E-14
zinc ion homeostasis (GO:0055069)	6.21E-14
cellular zinc ion homeostasis (GO:0006882)	6.27E-14
detoxification of inorganic compound (GO:0061687)	6.78E-14
stress response to copper ion (GO:1990169)	4.67E-12
detoxification of copper ion (GO:0010273)	5.60E-12
cellular response to zinc ion (GO:0071294)	4.26E-11
response to zinc ion (GO:0010043)	6.08E-11
cellular transition metal ion homeostasis (GO:0046916)	1.11E-10
cellular response to copper ion (GO:0071280)	1.16E-10

GO biological process	FDR
stress response to metal ion (GO:0097501)	4.09E-04
detoxification of inorganic compound (GO:0061687)	5.45E-04
stress response to copper ion (GO:1990169)	5.96E-04
cellular response to zinc ion (GO:0071294)	7.19E-04
cellular response to copper ion (GO:0071280)	1.12E-03
detoxification of copper ion (GO:0010273)	1.19E-03
cellular zinc ion homeostasis (GO:0006882)	1.25E-03
zinc ion homeostasis (GO:0055069)	1.40E-03
cellular response to cadmium ion (GO:0071276)	1.45E-03
response to copper ion (GO:0046688)	2.11E-03

Figure S7: Relative expression of selected miRNAs, as quantified by RT-PCR. Seq denotes expression as determined by small RNA sequencing while qPCR denotes the relative expression determined via real time PCR. Real time PCR expression was determined relative to endogenous RNU48 expression. Y-axis is log2-transformed, normalized count data from small RNAseq, and log2-transformed relative qPCR expression using the ddCt method. Error bars indicate mean and SEM from three (smallRNAseq) or four (qPCR) replicates.